Dynamics of Balanced Parentheses, II. 4D Dyck Triangle and Its Projections

Gennady Eremin

argenns@gmail.com

December 31, 2017

Abstract. In this article, we dissect the well-known Dyck triangle. We show that the classic Dyck triangle, the Catalan triangle, and the Catalan convolution matrix [5] are 2D projections of the 4D Dyck triangle. In the Dyck path, each node can be associated with four parameters: (1) the current character position i in the parentheses, (2) the imbalance j or an excess of left parentheses over right ones, (3) the index n of the associated Catalan number, and (4) the index k of the corresponding Dyck square (see [1]). These parameters are related by the equalities $i = n + k$, $j = n - k$. We consider all six 2D Dyck triangles and all four 3D projections in different lattices.

Key Words: Dyck words, Dyck path, Dyck triangle, Catalan convolution matrix.

Based on the version 2015 (in Russian)

This work is based continues a series of articles on the dynamics of Dyck words. The cycle includes the following papers:

Dynamics of balanced parentheses, I. Dyck squares [1].
Dynamics of balanced parentheses, II. 4D Dyck triangle and its projections.
Dynamics of balanced parentheses, III. Identification of Dyck words.
Dynamics of balanced parentheses, IV. Dyck polynomials.

In discrete mathematics are well-known 3D Pascal pyramid. In this article, we consider the Dyck paths in the multidimensional Dyck triangles.

1 Introduction

Recall, a Dyck path of length $2n$ (*semilength n* or *size n*) is a diagonal lattice path from the origin to node $(2n, 0)$ consisting of n upsteps in the form of vectors $(1, 1)$ and n downsteps in the form of vectors $(1, -1)$, such that the path never goes below the ground level. In the bracketed form, the left parenthesis corresponds to the upstep, and the right parenthesis is the downstep.

Figure 1 collected several pictures from [2]. In the grid, the *positions* of the diagonal vectors are plotted along the abscissa axis, *i-axis*, and the *unbalance* (exceeding the number of upsteps above downsteps) is along the ordinate axis, *j-axis*. Arrows show valid vectors. Diagonal vectors bypass accessible nodes, for which the sum of the coordinates is even. In the ith position, the unbalance j cannot exceed i, so we have a triangular design in the $i\times j$ grid, which we will call a *Dyck ij-triangle*. Thus, the node (i, j) (or *ij-node*) belongs to the Dyck ij-triangle if and only if

$$j \le i \quad \text{and} \quad i + j = \text{even}. \tag{1}$$

Each ij-node has a certain label (or *dynamics*) $d(i,j)$, which is equal to the number of paths starting at $(0, 0)$ and ending at (i, j). For any ij-node, the dynamics is determined as follows:

$$d(0, 0) = 1, \; d(i,j) = d(i-1, j+1) + d(i-1, j-1). \tag{2}$$

The dynamics is zero in unreachable nodes (condition (1) is not satisfied). In figure 1, in yellow we have identified three *ij*-nodes associated by (2) $d(7,1) = d(6,2) + d(6,0)$.

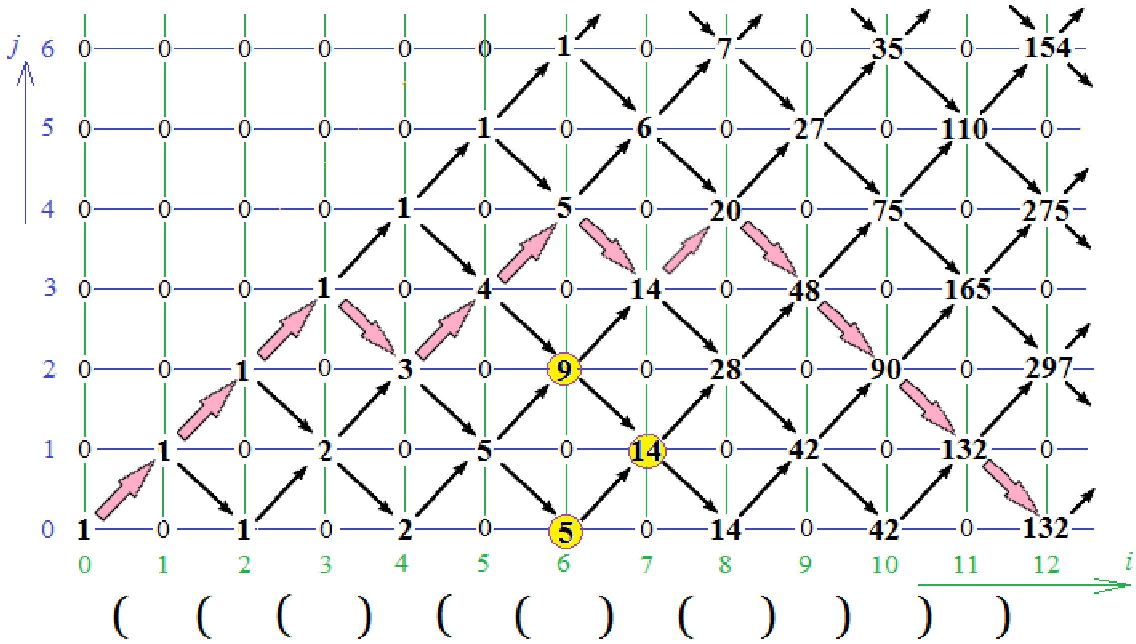

Figure 1. A Dyck path with its Dyck word.

In the lower two lines, we have the Catalan numbers, that is, $\mathrm{Cat}(n) = d(2n,0) = d(2n-1,1)$.

As an illustration, the Dyck *ij-path* of size 6 is shown by thick colored arrows, below the *i*-axis is the corresponding parentheses (the Dyck word of semilength 6). This path and the selected three *ij*-nodes will be repeated in following figures.

2 Isolines of Dyck triangle

Any rectangular coordinate system has horizontal and vertical lines or *isolines*. In Figure 1, horizontal lines are *j-isolines*, since all nodes (accessible and inaccessible) of the horizontal have the same *j* coordinate. Accordingly, the vertical lines are *i-isolines*, since the nodes of any vertical have the same *i* coordinate. In this section, we will consider additional isolines in the Dyck *ij*-triangle.

Accordance to (1) for a reachable node (i, j) the value of $i+j$ is even. Let's clarify this as follow: $i+j = 2n$. Consider a small example.

Example 1. In the Dyck *ij*-path (see Figure 1), the last four downward vectors pass through five nodes on a diagonal section from $(8, 4)$ to $(12, 0)$. For nodes of the falling diagonal starting at the top $(6, 6)$, the sum of the coordinates is $12 = 2\times 6$. The dynamics of the lower diagonal point is equal to the 6th Catalan number, $\mathrm{Cat}(6) = d(12,0) = 132$, and it is logical to connect such a diagonal with the 6th Catalan number, or rather with its index 6. For example, we can say that the node $(7, 5)$ is tied to $\mathrm{Cat}(6)$, meaning that $(7+5)/2 = 6$. □

The falling diagonal of the Dyck *ij*-triangle will be called an *n-isoline*. But in the triangle, there are also rising diagonals. It is easy to see that condition (1) implies the following: for any reachable node (i, j) the value of $i-j$ is even or zero. Let's concretize this so $i-j = 2k$. Consider another example.

Example 2. In the same Dyck *ij*-path, the first three upsteps pass through four nodes from (0, 0) to (3, 3) at the beginning of the main diagonal. For nodes of this rising diagonal, $k = 0$. The following ascending vectors pass through points (4, 2), (5, 3), and (6, 4) for which $k = 1$. In other words, we can say that these points are on the rising diagonal #1. For an achievable node, the ordinal number of the rising diagonal is equal to the half-difference of the coordinates. □

The rising diagonal of the Dyck *ij*-triangle will be called a *k-isoline*. As a result, we can say that any accessible node (v, w) is at the intersection of four isolines: (1) the *i*-isoline #*v* (vertical), (2) the *j*-isoline #*w* (horizontal), (3) the *n*-isoline number $(v+w)/2$ (falling diagonal), and (4) the *k*-isoline number $(v-w)/2$ (rising diagonal). Four isolines #0 intersect at the origin.

Now, for the attainable node (i, j), we can rewrite (1) in the form

$$i+j=2n,\ \ i-j=2k \quad \text{or} \quad i=n+k,\ \ j=n-k \quad (i, j, n, k \geq 0). \tag{3}$$

Let’s transform Figure 1 by removing the useless inaccessible nodes with zero dynamics. In Figure 2, we showed the yellow *n*-isolines from #0 to #8. The yellow arrow shows the direction of the virtual *n*-axis. In red, we showed the *k*-isolines from #0 to #6. The red arrow shows the direction of the virtual *k*-axis. It is easy to see that inequalities

$$i \geq n \geq j,\ \ n \geq k$$

follow from (3). And this is checked directly on the picture. Here we have repeated the Dyck *ij*-path and the three selected *ij*-nodes.

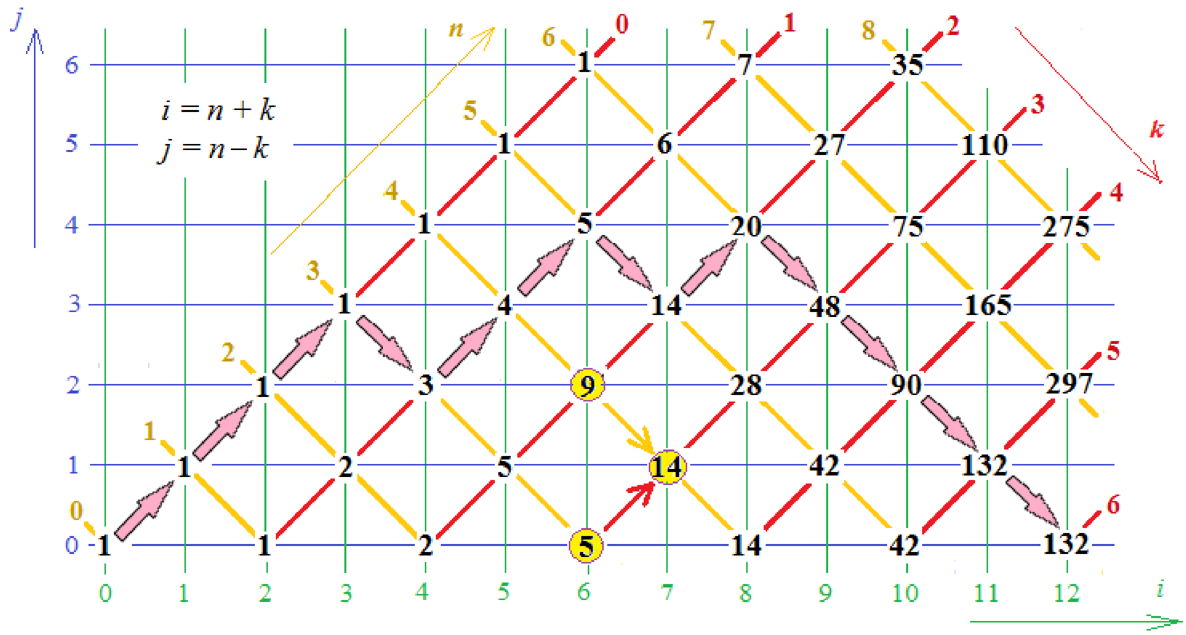

Figure 2. The Dyck *ij*-triangle.

We pay attention to the fact that the Dyck paths pass only diagonals, that is, *n*-isolines and *k*-isolines. The upsteps lie on the *k*-isolines, and the downsteps lie on the *n*-isolines.

Let's give a concrete meaning to the variable k from (3). Any node (v, v), $v > 0$, is the intersection of *i*-isoline #*v*, *j*-isoline #*v*, *n*-isoline #*v*, and *k*-isoline #0. It is easy to prove (see [1])

$$\text{Cat}(v) = d^2(v, v) + d^2(v, v-2) + d^2(v, v-4) + \ldots + d^2(v, v-2\lfloor v/2 \rfloor) \tag{4}$$

or

$$\mathrm{Cat}(v) = \sum_{k=0}^{\lfloor v/2 \rfloor} t_k^2(v), \;\; t_k(v) = d(v, v-2k).$$

In (4), the terms are logically called Dyck squares. Some terms are obvious, for example,

$t_0(v) = d(v, v) = 1;$ $t_1(v) = d(v, v-2) = v-1;$ $t_2(v) = d(v, v-4) = v(v-3)/2;$ (5)
$t_{\lfloor v/2 \rfloor}(v) = d(v, v-2\lfloor v/2 \rfloor) = \mathrm{Cat}(\lceil v/2 \rceil).$

In this case, the variable k is the index of the Dyck square. Thus, all four considered isolines are related to certain attributes (states) of balanced parentheses. Let's call i, j, n, k *coordinate variables*, and hence the dependences (3) are the *coordinate equations*.

So, we are dealing with 4-dimensional object, the *Dyck ijnk-triangle*. As a result, we can write the dynamics equation (2) in a general form (for four-dimensional space):

$$D(0,0,0,0) = 1, \;\; D(i, j, n, k) = D(i-1, j+1, n, k-1) + D(i-1, j-1, n-1, k). \quad (6)$$

The 4D Dyck triangle can have up to six different 2D projections, one of which is presented in Figure 2. In the Dyck *ij*-triangle, the *i*-isoline #0 and the *j*-isoline #0 are coordinate axes, and these axes can be replaced. In the next section, we consider a known matrix, which is another 2D projection of the Dyck *ijnk*-triangle.

3 Catalan convolution matrix and Dyck *nj*-triangle

Several years ago, the author of this article had to pack the Dyck *ij*-triangle in the computer's memory [3]. In such a triangle, nodes with zero dynamics (unreachable nodes) are ballast. After removing these nodes, we reduce the array by half.

In Figure 2, let's rotate all *n*-isolines to the vertical position around the top points; as a result, only the achievable nodes remain in the array. Figure 3 shows a new 2D projection in the $n \times j$ grid (*i*-axis is replaced by *n*-axis). Let's call this projection the *Dyck nj-triangle*.

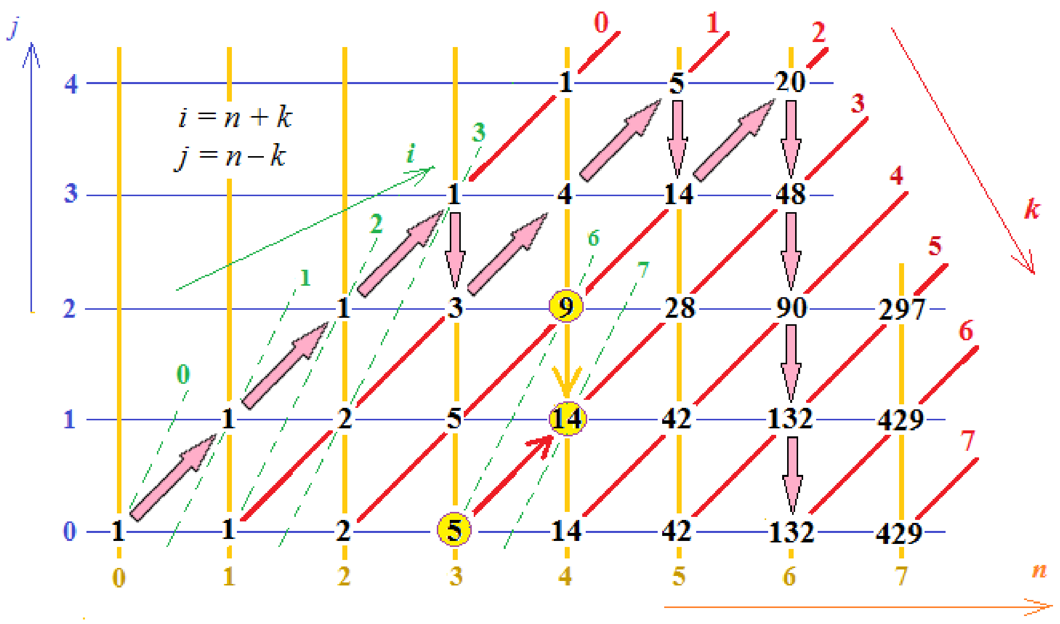

Figure 3. The Dyck *nj*-triangle.

We see that *i*-isolines practically disappeared from the grid. For orientation in Figure 3, we have connected some *nj-nodes* with dotted *i*-isolines and conditionally showed the direction of the virtual *i*-axis (recall the coordinate equation $i = n + k$). As we see the former path has significantly changed; in the new Dyck *nj-path* the downsteps are transformed into breaks. As a result, the length path was halved.

In the new projection on the abscissa axis, we indicate the index of the associated Catalan number, so you can not apply the dynamics equation (2) to the *nj*-nodes. However, the generalized equation (6) is applicable in all projections (and not only two-dimensional). For the selected *nj*-nodes, we can write

$$D(7, 1, 4, 3) = D(6, 2, 4, 2) + D(6, 0, 3, 3). \tag{7}$$

The equality (7) is universal for all projections, as well as for the Dyck *ijnk*-triangle, so we will not give it any more, except to refer to it.

Let's define the relationship between the items of the Dyck *ij*-triangle and the Dyck *nj*-triangle (or between *ij*-nodes and *nj*-nodes). The Dyck *nj*-triangle is known in the literature as the Catalan convolution matrix [4, 5]. Elements of this matrix (and correspondingly elements of the Dyck *nj*-triangle) are defined as follows [5, p. 2928]:

$$C(n, j) = \binom{2n-j}{n-j} - \binom{2n-j}{n-j-1}, \quad n, j \geq 0.$$

Next, let us use the coordinate equations (3) to obtain the general term of the Dyck square (in addition to (5)):

$$t_k(i) = C(n, j) = C(i-k, i-2k) = \binom{i}{k} - \binom{i}{k-1}. \tag{8}$$

A detailed analysis of (8) is made in [1]. As we see, the use of different projections of the Dyck *ijnk*-triangle, can simplify some calculations.

4 Lattice paths in $n \times n$ grid and Dyck *nk*-triangle

In the considered projections (see Figures 2 and 3), at each *ijnk*-node of the form $(i, 0, n, k)$ the last two coordinates are the same, that is, $n = k$. This follow from (3), and therefore it is true for any (not only two-dimensional) projection and, in particular, for the Dyck *nk*-triangle. This means that in the Dyck *nk*-triangle the *j*-isoline #0 is the main diagonal. In this case, we get a lattice with $n \times n$ (or $k \times k$) square cells. Such square diagrams are well known [6, 7].

Let's transform the Dyck *ij*-triangle in Figure 2. We twirl the diagram around the main diagonal 180 degrees (change axes) and then rotate clockwise by 45 degrees. As a result, we formed the Dyck *nk*-triangle (see Figure 4). In a new projection, the diagonals became horizontal and vertical lines. The same Dyck *nk*-path is the monotonic lattice path along the edges of the *nk*-grid.

In the Dyck *nk*-triangle, the arbitrary Dyck *nk*-path starts in the lower left corner, finishes in the upper right corner, and consists entirely of edges pointing rightwards or upwards. Such a path from (0, 0) to (n, n) (or (k, k)) does not pass above the main diagonal $n = k$.

In Figure 4, the usual square lattice is complemented by diagonal *i*-isolines and *j*-isolines for better orientation at the grid nodes. For example, it is easy to verify the dynamic equation (6) for three selected nodes.

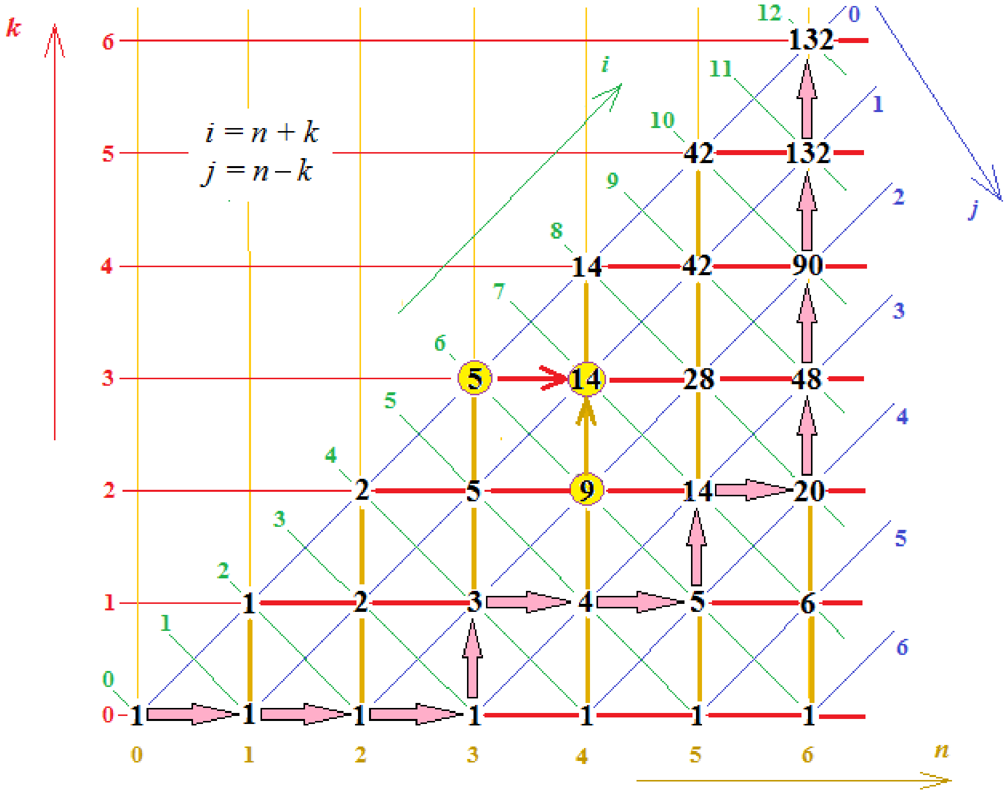

Figure 4. The Dyck *nk*-triangle.

Let's pay attention to the following. All three described triangles are well known and studied in detail. The first two grids $i \times j$ and $n \times j$ have the clear and natural coordinates. We have another situation with the classic square lattice $n \times n$. Here both coordinates are intuitively related to the Catalan number index and do not differ. But this is not possible; on the plane, each coordinate axis serves a certain quantitative characteristic of the object.

In our case, on the abscissa we indicate the index of the associated Catalan number; the ordinate is the index of the Dyck square. So by means of the Dyck *ijnk*-triangle and coordinate equations (3), we distinguish and identify axes of the square lattice.

5 Other 2D Dyck triangles

In the Dyck *ijnk*-triangle, each node is uniquely determined by any pair of coordinate variables, and the other two coordinates are computed from (3). This means that all two-dimensional (and also three-dimensional) projections are equivalent, mutually interchangeable. For example, we can easily move from the Catalan convolution matrix (the Dyck *nj*-triangle) with traced Dyck paths to the traditional Dyck *ij*-triangle, on which we will see the same paths. Obviously, to solve a certain range of problems, this or that projection is preferred.

We have considered three known two-dimensional projections of the Dyck *ijnk*-triangle; the author of this article did not see other projections. There are three more projections in the following coordinate grids: $i \times n$ (or $n \times i$), $i \times k$ (or $k \times i$), and $k \times j$ (or $j \times k$). We can assume that these projections are not yet in demand.

5.1. The Dyck *in*-triangle. In Figure 5, we have traditionally indicated the position of the brackets along the abscissa axis, and the ordinate axis is the index of the associated Catalan number. The resulting Dyck *in*-triangle is more like a wedge, not a triangle.

Here *j*-isolines are not shown, so as not to obscure the drawing. The lower nodes (Catalan numbers) of the *k*-isolines are on the *j*-isoline #0. The next group of nodes (more Catalan numbers) is on *j*-isoline #1 and so on.

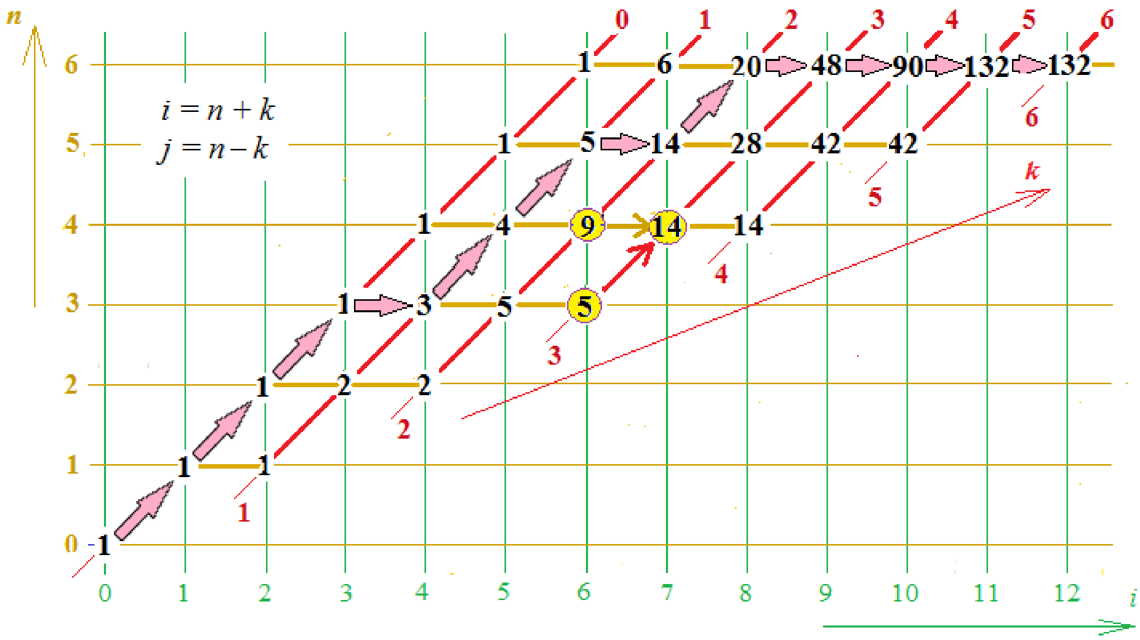

Figure 5. The Dyck *in*-triangle.

5.2. The Dyck *kj*-triangle. In Figure 6, we have traditionally indicated the unbalance of the brackets along the ordinate axis, and the abscissa axis is the index of the Dyck square. In fact, the resulting Dyck *kj*-triangle can no longer be called a triangle, since the entire first quadrant is accessible to Dyck paths (there are no forbidden areas).

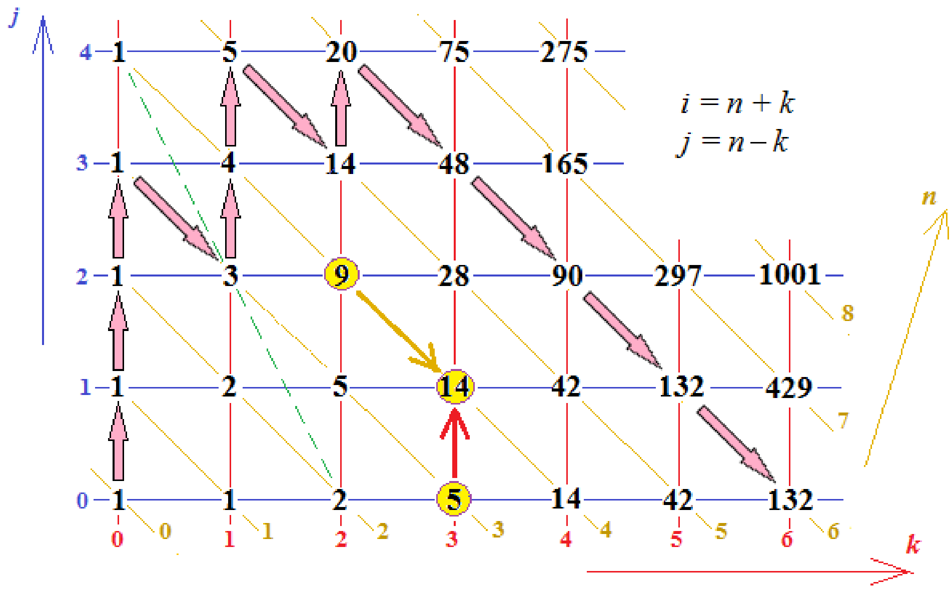

Figure 6. The Dyck *kj*-triangle.

It also does not show all isolines. Nodes lying on the same *i*-isoline are sufficiently far from each other. For example, the green dashed line, *i*-isoline #4, links *kj*-nodes (0, 4), (1, 2), and (2, 0). Recall, in accordance with the coordinate equations $i = j + 2k$.

5.3. The Dyck *ik*-triangle. In Figure 7 on the abscissa axis, we indicated the usual bracket positions, and the ordinate axis is the indices of the Dyck square. The resulting picture is a somewhat unusual triangle. Not all isolines are shown in the Dyck *ik*-triangle. On the whole scheme we have drawn only the *j*-isoline #0 (dotted blue line) which connects the Catalan numbers. As we see, the Catalan numbers are the upper elements of the columns.

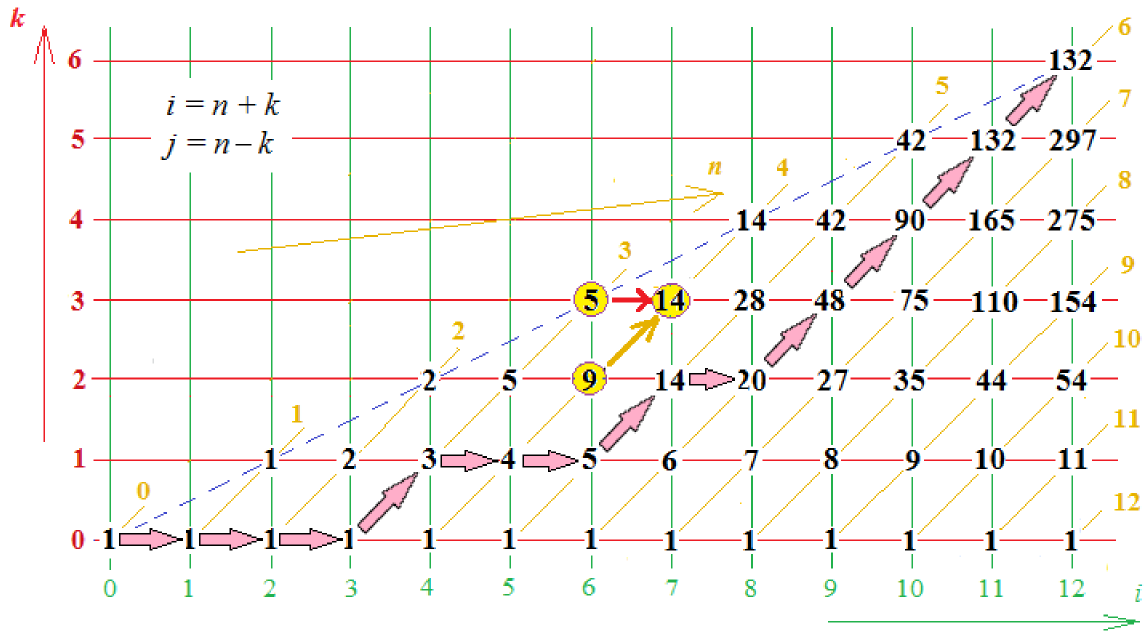

Figure 7. The Dyck *ik*-triangle.

Let us pay attention once again, in all projections of the 4D *ijnk*-triangle, isolines with zero number intersect at the origin.

6 3D Dyck triangles

In this section, we construct 3D projections of the Dyck *ijnk*-triangle. In total there are four three-dimensional projections, since we believe that the order of the axes does not matter. For example, we do not distinguish between lattices $i \times j \times n$, $i \times n \times j$, $j \times n \times i$, $j \times i \times n$, $n \times i \times j$, and $n \times j \times i$. We will only choose the most convenient image.

In the general case, if possible, we will adhere to the order of the coordinates in the $i \times j \times n \times k$ lattice. Let's hope that this will simplify the transition from the selected three-dimensional projection to the four-dimensional design.

It is convenient to create a 3D projection based on some selected 2D triangle. For example, from the *ij*-triangle (see Figure 2) we can get the *ijn*-triangle or the *ijk*-triangle. Accordingly, adding one coordinate in the *nk*-triangle (see Figure 4), it is not difficult to construct the *ink*-triangle or the *jnk*-triangle.

For a better orientation in the three-dimensional projections, we will mark rays indicating all four coordinates of the points on these rays. This applies to the axes and to different diagonals. In the rays, certain coordinates of the points can be the same, some coordinates are fixed. In case of coincidence of coordinates, the first variable is repeated. Here are a few examples:

(*i*, 0, 0, 0), (0, *j*, 0, 0), (0, 0, *n*, 0) и (0, 0, 0, *k*) – the main axes in the 4D lattice;
(*i*, *i*, *i*, 0) – the central ray in the 3D Dyck *ijn*-triangle (or *k*-diagonal #0);

(i, j, j, 0) – the main diagonal in the Dyck nj-triangle (see Figure 3);
(i, 4-i, 2, i-2) – the n-diagonal #2 in the Dyck ijn-triangle (see the following figure).

In the drawings, the isolines are shown in the corresponding color:

i-isolines – green,
j-isolines – blue,
n-isolines – dark yellow,
k-isolines – red.

In projections, we will also repeat the coordinate equations (3), the old Dyck path, and the three nodes (6, 0, 3, 3), (6, 2, 4, 2), (7, 1, 4, 3). We recall the equation of dynamics for these nodes D(7, 1, 4, 3) = D(6, 0, 3, 3) + D(6, 2, 4, 2)

6.1. The Dyck *ijn*-triangle. The Figure 8 shows an $i \times j \times n$ lattice, that based on the Dyck ij-triangle. As we see the Dyck ijn-triangle is flat as all previous projections. This is not surprising since the coordinate equations (3) are linear.

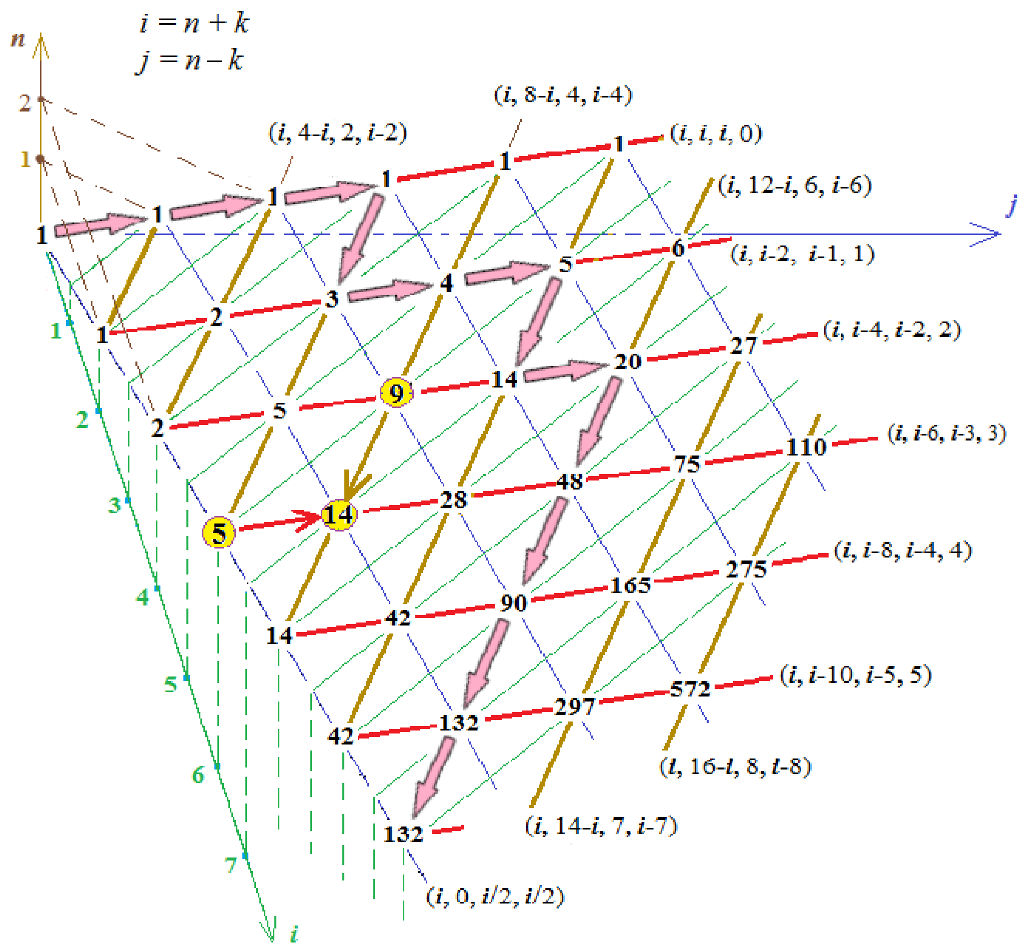

Figure 8. The Dyck ijn-triangle.

6.2. The Dyck *ijk*-triangle. The Figure 9 shows an $i \times j \times k$ lattice, that also based on the Dyck *ij*-triangle. As we see the Dyck *ijk*-triangle is flat.

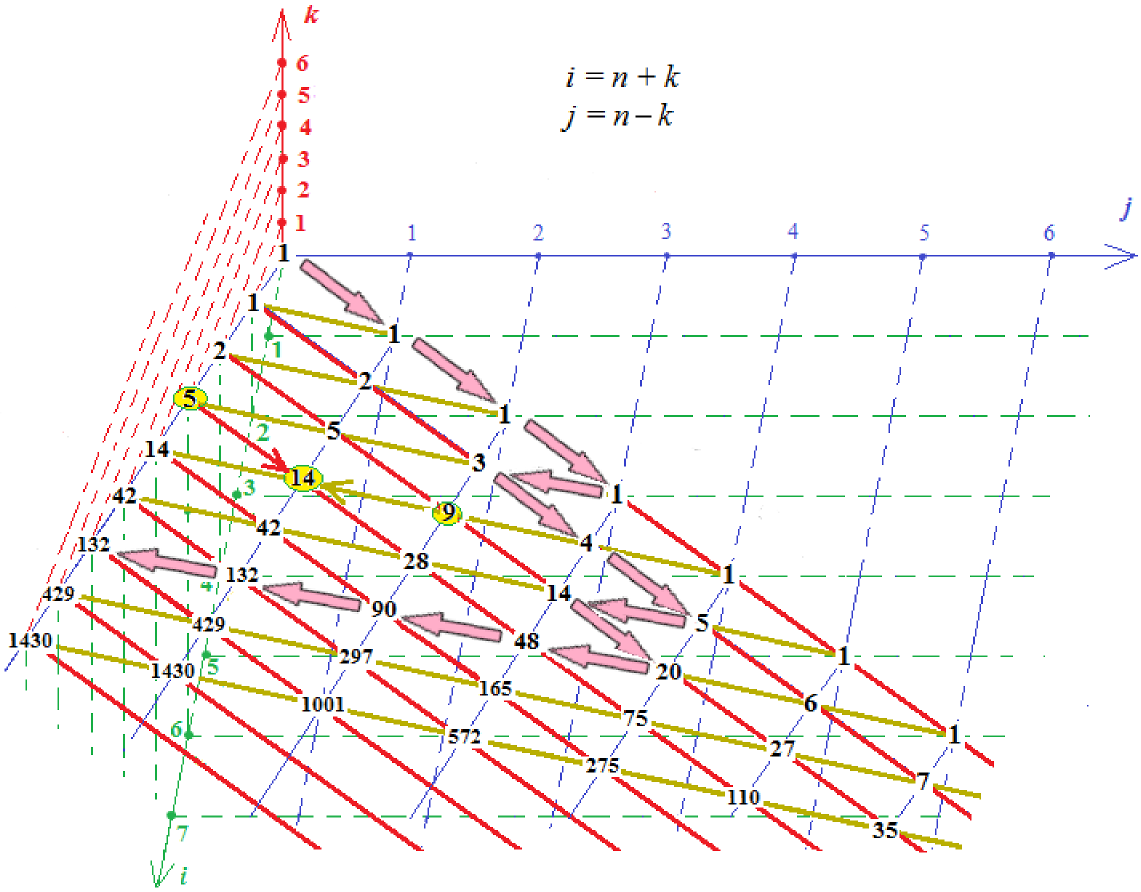

Figure 9. The Dyck *ijk*-triangle.

6.3. The Dyck *nik*-triangle. The Figure 10 shows an $n \times i \times k$ lattice, that based on the Dyck *nk*-triangle (see Figure 4). This projection of the 4D Dyck *ijnk*-triangle is also flat.

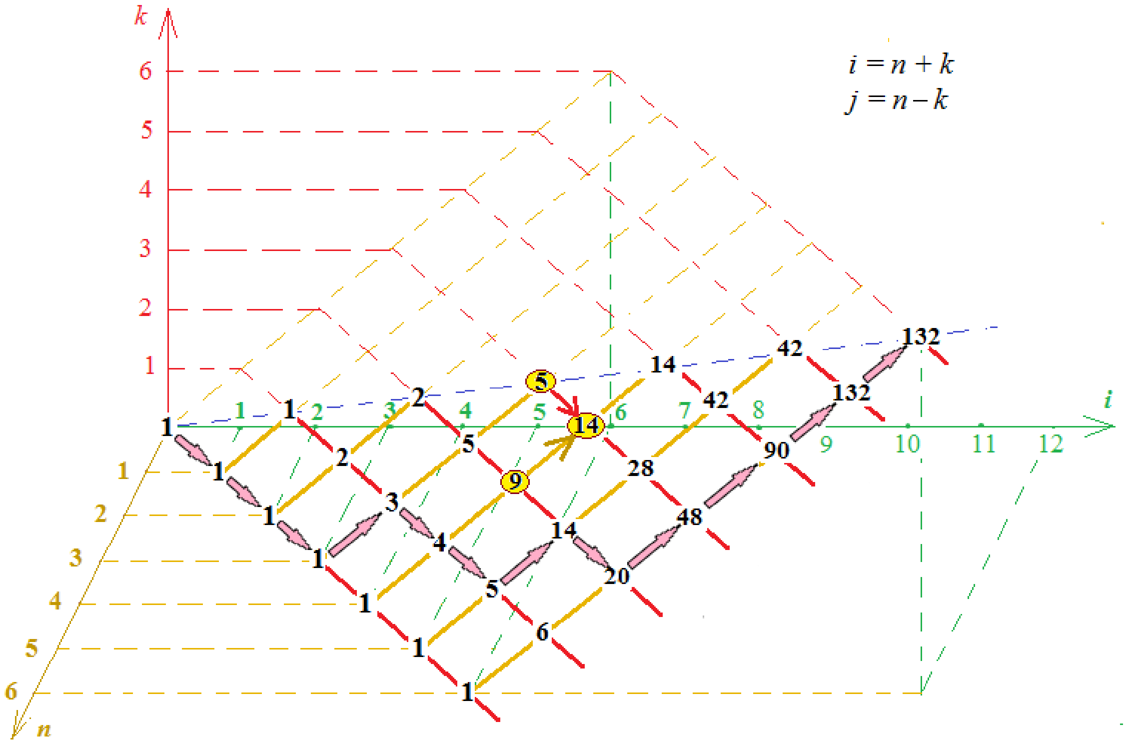

Figure 10. The *nik*-triangle.

6.4. The Dyck *jnk*-triangle. The Figure 11 shows an $j \times n \times k$ lattice, that also based on the Dyck *nk*-triangle (see Figure 4). This projection of the 4D Dyck *ijnk*-triangle is also flat.

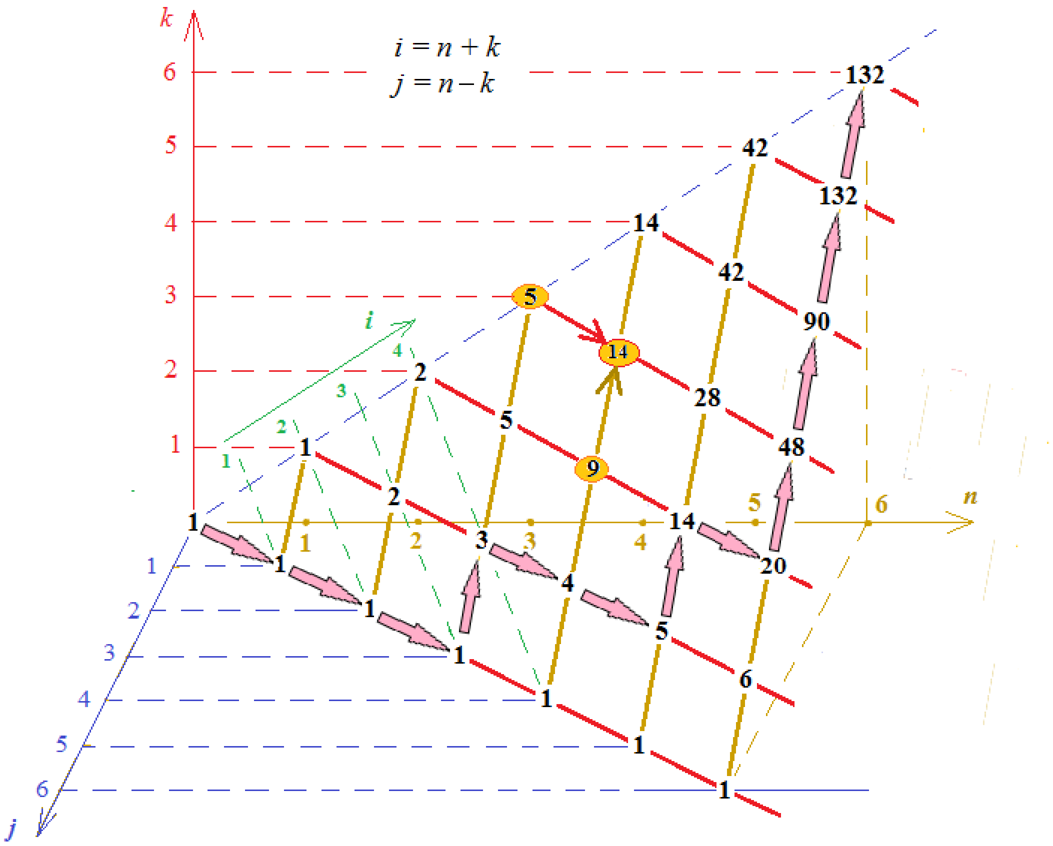

Figure 11. The Dyck *jnk*-triangle

The figure 11 shows roughly the direction of the fourth *i*-axis. Perhaps this drawing is most convenient to build a four-dimensional design.

References

[1] Gennady Eremin, "Dynamics of balanced parentheses, I. Dyck squares", 2017. http://eremin.xyz/dd1-Dyck_squares-2017.pdf

[2] Sergei K. Lando, "Lectures on Generating Functions", AMS, Providence RI, 2003. http://www.ams.org/books/stml/023/stml023-endmatter.pdf

[3] Геннадий Еремин, "Правильные скобочные последовательности и их динамика", 2015. http://eremin.xyz/dyck/modified-triangle/

[4] Verner E. Hoggatt, Jr., Marjorie Bicknell, "Pascal, Catalan, and General Sequence Convolution Arrays in a Matrix", *The Fibonacci Quarterly* 14, no. 2 (1976), 135–142. http://www.fq.math.ca/Scanned/14-2/hoggatt2.pdf

[5] David Callan, Emeric Deutsch, "The Run Transform", *Discrete Mathematics*, **312** (2012), 2927-2937. http://www.sciencedirect.com/science/article/pii/S0012365X12002233

[6] https://en.wikipedia.org/wiki/Catalan_number

[7] http://mathworld.wolfram.com/DyckPath.html